

This is the accepted manuscript made available via CHORUS. The article has been published as:

Structural Comparison of n-Type and p-Type $\text{LaAlO}_3/\text{SrTiO}_3$ Interfaces

Ryosuke Yamamoto, Christopher Bell, Yasuyuki Hikita, Harold Y. Hwang, Hiroyuki Nakamura, Tsuyoshi Kimura, and Yusuke Wakabayashi

Phys. Rev. Lett. **107**, 036104 — Published 15 July 2011

DOI: [10.1103/PhysRevLett.107.036104](https://doi.org/10.1103/PhysRevLett.107.036104)

Structural comparison of n -type and p -type $\text{LaAlO}_3/\text{SrTiO}_3$ Interfaces

Ryosuke Yamamoto¹, Christopher Bell², Yasuyuki Hikita², Harold Y. Hwang^{2,3,4},
Hiroyuki Nakamura¹, Tsuyoshi Kimura¹, and Yusuke Wakabayashi^{1*}

¹*Division of Materials Physics, Graduate School of Engineering Science,
Osaka University, Toyonaka 560-8531, Japan*

²*Department of Advanced Materials Science,
University of Tokyo, Kashiwa, Chiba 277-8561, Japan*

³*Japan Science and Technology Agency,
Kawaguchi, Saitama 332-0012, Japan*

⁴*Department of Applied Physics and Stanford Institute for Materials and Energy Science,
Stanford University, Stanford, California 94305, USA*

Abstract

Using a surface x-ray diffraction technique, we investigated the atomic structure of two types of interfaces between LaAlO_3 and SrTiO_3 , that is, p -type (SrO/AlO_2) and n -type (TiO_2/LaO) interfaces. Our results demonstrate that the SrTiO_3 in the sample with the n -type interface has a large polarized region, while that with the p -type interface has a limited polarized region. In addition, atomic intermixing was observed to extend deeper into the SrTiO_3 substrate at the n -type interface compared to the p -type. These differences result in distinct degrees of band bending, which likely contributes to the striking contrast in electrical conductivity between the two types of interfaces.

* e-mail: wakabayashi@mp.es.osaka-u.ac.jp

Characteristic physical properties that emerge at interfaces between two different compounds have long been attracting great attention. A well-known classic example is the semiconductor diode, while modern examples include anomalous conductivity[1] or superconductivity[2] found at heterointerfaces of metal oxides, large conductivity found at the interface of two insulating organic materials[3], and so on. Heterostructures of transition metal oxides are excellent playing-fields to study the behavior of electrons at interfaces because their wide variety of properties arising in isostructural materials is already established, as well as their lattice degree of freedom that allows the stabilization of various electronic states. One of the notable examples is the interface between two band insulators with the perovskite ABO_3 structure, $LaAlO_3$ (LAO) and $SrTiO_3$ (STO).[1, 4] The n -type interface, in which the LAO layer is grown on top of TiO_2 -terminated STO, has highly mobile carriers, while the p -type interface, in which the LAO layer is grown on top of SrO -terminated STO, is totally insulating.[1] To observe conductivity in the n -type interface requires a 4 unit cell-thick or thicker LAO layer.[5] The existence of this critical thickness is understood to support the role of the polar discontinuity in inducing this anomalous conductivity,[6] although x-ray photoemission studies have not found electric fields in the LAO.[7] Ref.[5] also reported that the application of an electric field perpendicular to the surface can switch the conductivity of the interface. Clear memory behavior was observed only in the films having 3-unit cell thickness, just below the critical thickness. This memory behavior also supports the idea that some kind of polarization plays a critical role in the anomalous conductivity.

Various theoretical studies have been performed on this system to understand the peculiar conductivity. In many cases, the interfacial structure is optimized in order to reduce the energies within the theories. As a result, various structures, i.e., large polarization in the LAO[8], large polarization in the STO with the polarization vector towards the surface[9], the substrate side[10], or polarization in both the LAO and STO[11] are proposed for both types of interfaces. Experimentally, a number of studies have been performed on the conductive n -type interfaces while the study on the insulating p -type interfaces has been extremely limited. Given the striking contrast between metal and insulator, while the growth parameters of the LAO are fixed, a differential study may greatly illuminate the origin of the different properties between the n -type and p -type interfaces. Therefore we have conducted surface x-ray scattering measurements, which allow us to obtain extremely high resolution images of both types of interface.[12]

Five-unit-cell thick LaAlO_3 ultrathin films were fabricated by means of pulsed laser deposition (PLD) at a temperature of 873 K, in an oxygen pressure of 1.33 mPa, with a laser fluence of 1.9 J/cm^{-2} . Prior to growth the samples were annealed at 1223 K for 30 mins in an oxygen environment of 0.67 mPa. The laser repetition rate was 2 Hz, and for the p -type sample 17 pulses were needed to deposit 1-unit cell of SrO prior to the LAO growth, as calibrated by *in-situ* reflection high-energy electron diffraction. After deposition both samples were annealed at the growth temperature for one hour at an oxygen pressure of $4 \times 10^4 \text{ Pa}$. X-ray diffraction measurements were performed at BL-3A of the Photon Factory, KEK, Japan. A standard four-circle diffractometer equipped with a scintillation counter is installed on this beamline. Measurements were made in air at room temperature with 12 keV x-rays. For the n -type and p -type samples, four and six crystal truncation rods (four inequivalent rods for both samples) were measured with rocking curve measurements. No radiation damage was observed during the data collection.

X-ray scattering intensity per unit illuminated area along the (00ζ) and (01ζ) lines for both samples are shown in Figs. 1(a), (b), (d), and (e). Throughout this paper, we use the reciprocal lattice defined by the substrate crystal lattice. There are sharp Bragg peaks from the substrate at integer ζ positions as well as broad features due to the LAO film. The periodic undulation in intensity reflects the thickness of the film. The overall resemblance between the intensity distributions for the two samples is due to the same averaged perovskite lattice, while the slight variations between them contain the crucial information about the structural differences.

In order to obtain the real space structure of the interfaces, we performed an electron density analysis by following the phase retrieval process known as COherent Bragg Rod Analysis (COBRA).[13, 14] The depth dependences of the electron densities obtained by this analysis on (00ζ) rods are shown in Figs. 1 (c) and (f). The peaks with alternating heights correspond to the AO (higher peaks) and BO_2 (lower peaks) planes. The origin of the horizontal axis is chosen to lie at the first monolayer of the LAO. The nominal interface is thus just to the left of the origin, with the peaks in the negative z region belonging to the nominal substrate, and the peaks between $z = 0$ and 23\AA are due to the nominal LAO region. The flat and very low electron density beyond the sample, $z > 23\text{\AA}$, corresponds to the air region. The surface layers of the samples are, as expected, the BO_2 plane for the n -type sample and the AO plane for the p -type sample.

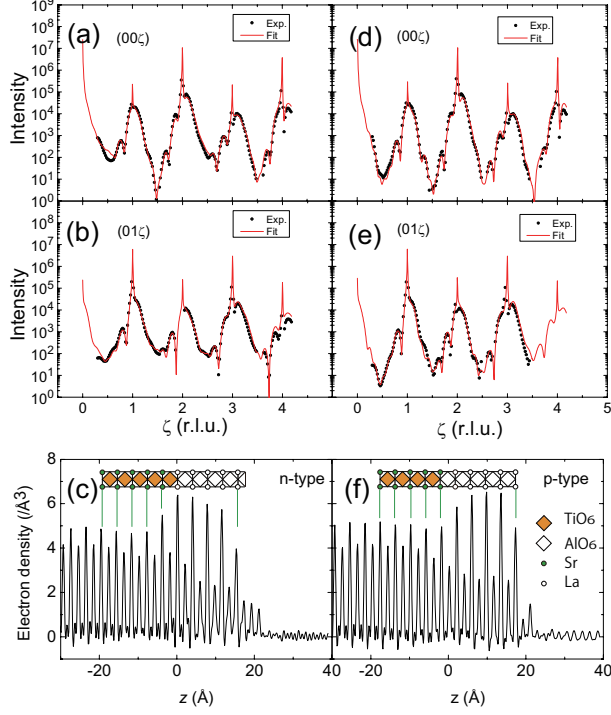


FIG. 1: (Color online) X-ray scattering intensity profiles along (a) the (00ζ) -line and (b) the (01ζ) -line for the *n*-type sample. Closed symbols show the experimental results, and the solid curves show the result of the least squares fitting. The depth profile of the electron density, obtained from the electron density analysis performed on the (00ζ) rod, is shown in (c). Panels (d)-(f) show those for the *p*-type sample.

First, we examine the depth profiles of the electron density. The peak shifts from the average STO lattice for the *n*-type and the *p*-type samples as functions of the depth are shown in Fig. 2(a) with closed and open symbols, respectively. The nominal interface is labeled by thick vertical line, and the shaded area represents the region having smaller atomic occupancies. The decrease of Δz with increasing z observed in the LAO region is due to the smaller lattice parameter of LAO. There is a significant expansion of the STO cell volume around the interface. This expansion for the *n*-type sample was reported in ref.[14] and was attributed to the change in the valence of Ti ions. Our analysis clearly shows the same amount of volume expansion around the interface in both samples, which seems to imply a common origin of the expansion. Since the valence of the Ti ions around *p*-type interfaces is known to be constant[15], the volume expansion in both interfaces should not be attributed to the change in the valence of Ti ions. Instead, these expansions can be caused

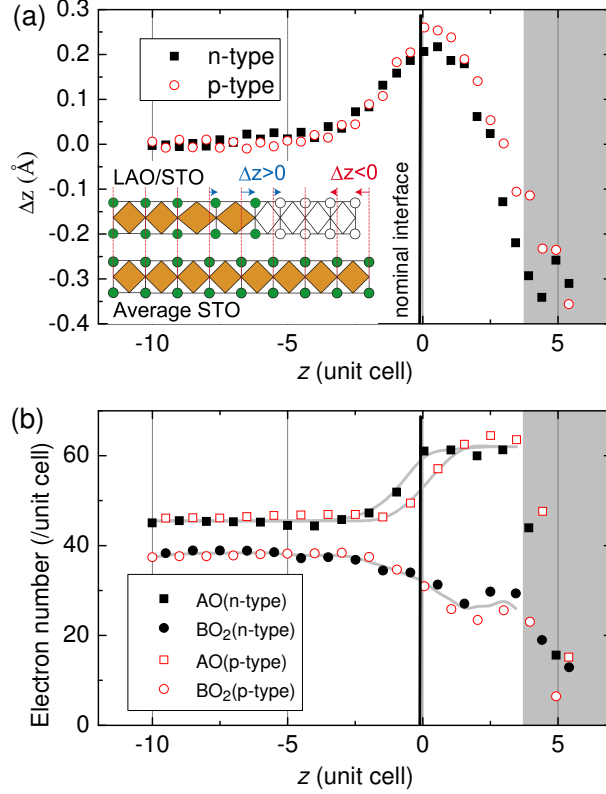


FIG. 2: (Color online) (a) The depth dependence of the positions of the peaks shown in Figs.1(c) and (f) presented as the shift from the average STO lattice. Positive is defined as toward the surface. (b) The number of electrons for each peak in Figs. 1 (c) and (f) as a function of depth. The gray curves are guides to the eye. The shaded areas for both panels show the region having small atomic occupancy.

by oxygen vacancies, or small changes in the cation stoichiometry. For example, according to ref.[16], 1 % of Sr deficiency causes a 0.06\AA expansion of the c -axis, which is comparable to the observed value.

Figure 2(b) shows the number of electrons for each peak in Figs. 1 (c) and (f) as a function of depth. The uncertainty of these plots estimated from the undulation of the electron density in the air-region in Figs. 1 (c) and (f) is on the order of the symbol size. For the two samples, one can easily see that the depth dependence of the electron number of the BO₂ planes is almost the same, while for the AO planes it is quite different: the midpoint of the AO interface for the n -type interface is deeper than that for the p -type interface by about one unit cell. This structure can be realized by the removal of Sr ions beneath the topmost TiO₂ layer of the n -type STO during the annealing or growth. [17]

The difference between the n -type and p -type interfaces indicates that the origin of this ionic substitution is related to the polarity of the interface, since if the penetration of the La ions observed in the n -type sample is purely a result of an inertial effect, the same atomic penetration should be observed in the p -type sample. This atomic mixing makes a one unit cell thick (La,Sr)TiO₃ layer at the n -type interface as reported in ref.[14], whereas the p -type sample does not have such a layer. Based on this difference in occupancy, the formation of the conductive (La,Sr)TiO₃ at the n -type interface has been discussed as the origin of the conduction in this interface. However, we stress that this type of stoichiometric interdiffusion cannot solve the polar discontinuity problem, and this difference is also less likely to show significant thickness dependence or memory behavior[5], which implies a significant role of the polarization in the system. In order to find differences in the polarization between the two types of interfaces, we performed a least squares structure refinement.

The least squares analyses were performed on the measured intensities to refine the positions of the A-site ions, the B-site ions, the O1-site ions, (which belong to the AO-planes), and the O2-site ions (in the BO₂-planes). The initial values of the atomic occupancy parameters for the metal sites were determined to reproduce the electron numbers shown in Fig. 2(b), assuming the occupancies of the O1 and O2 sites are unity, except for the one unit cell on the surface. These occupancy parameters were fixed during most of the analysis, and refined in the very last cycle of the refinement. Isotropic atomic displacement parameters were fixed to 0.4 Å². Tilting and rotation of the BO₆ octahedra are neglected in order to reduce the number of fitting parameters. The error bars of the atomic positions were estimated with a threshold of 3 % increase in the total squared error.

Figure 3 (a) shows the atomic displacements from the substrate STO lattice observed in the n -type sample. Positive displacement represents the atomic movement towards the surface. As is observed in this figure, around the interface the A, B, and oxygen sites displace towards the surface, and the overall feature is similar to previous reports.[14, 18, 19] The oxygen atoms in the STO region displace toward the surface about 0.06 Å more than the cations, meaning that a polarization arises there. This oxygen displacement lasts far deeper than the cation displacement, indicating that the polarized region spreads far into the STO. In the LAO region, by contrast, the O1 atoms lie relatively lower than the metals ions, while the O2 atoms displace the other way, showing little polarization. In order to better represent the local polarization, the displacements of metal ions and oxygens averaged over a unit cell

are also plotted in Fig. 3 (a). Inward polarization (and thus the electric field) of STO is clearly observed. The local electric field is proportional to the slope of the electron potential. A schematic band diagram expected from the electric field distribution is also presented in the right hand side of the same panel. The electric field extends far inside of STO producing a large change in the potential energy of the electrons at the interface. This result shows good agreement with previously reported photoemission spectroscopy (PES),[20] which reports 0.25 eV of band bending corresponding to an inward electric field in the STO region for the *n*-type sample. They attributed the metallic conduction to this band bending. Polarization in the STO is not reported in a previous surface diffraction study on an *n*-type interface,[18] however the origin of this discrepancy is unclear. Quantitatively the oxygen displacement observed in the STO region is very close to the value predicted by theoretical calculations[10] for 2 to 3 nm away from the interface. Very close to the interface, theory predicts a much larger polarization, however this discrepancy may be caused by atomic mixing, which is not taken into account in the theoretical work. In the *n*-type interface, La^{3+} ions substitute Sr^{2+} ions in the STO region as shown in Fig. 2(b). Such migrated La^{3+} ions produce an electric field that cancels the inward one at the interface.

Figure 3 (b) shows the atomic displacements in the *p*-type sample. Overall the observed features are similar to those in the *n*-type sample. The maximum value of the A-site ion deviation is 0.25 Å, which is very close to the value for the *n*-type sample. The B-site ion displacement towards the surface was larger than for the A-site ions, in qualitative agreement with the *n*-type interface. Quantitatively however, the B-site displacement, 0.09 Å more than the A-site, is twice as large as that for the *n*-type system. Despite this, over the relatively short space of 3 unit cells these atomic shifts recover, leading to larger, but more localized, displacements in the *p*-type sample. Turning our attention to the oxygen atoms, little polarization is observed in the LAO region, similar to the *n*-type case. In the STO region close to the interface, oxygen ions displace significantly toward the surface, which implies the same polarity as in the *n*-type sample. Again, however, the larger displacement of the oxygen ions is more localized at the interface, and a noticeable polarization was found within only a 4 unit cell thick region, leading to a polarized region in the *p*-type sample that is narrower than in the *n*-type sample. The contrast in the polarization distribution reflects the difference in the electric field, which will result in different degrees of band bending. A schematic band diagram for the *p*-type interface is presented in Fig. 3 (b). Although the

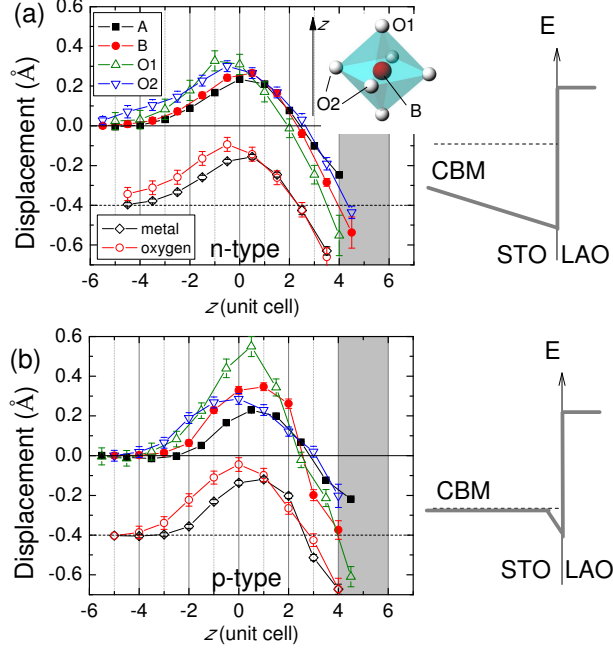


FIG. 3: (Color online) Atomic positions for (a) the *n*-type sample, and (b) the *p*-type sample. The abscissa origins are taken at the nominal interface, with positive direction pointing toward the LAO. Shaded areas represent regions having small occupancy. Positions of metal ions (open diamonds) and oxygens (open circles) averaged over a unit cell are also plotted with a shift of -0.4 \AA to show the local polarization. Significant polarization was observed in the STO region, corresponding to $z < 0$. Schematic band diagrams are also presented. The conduction band minimum (CBM) energy (E) of the bulk STO is marked with a horizontal dashed line.

local electric field around the interface in the *p*-type sample is twice as intense as that in the *n*-type sample, the short screening depth makes the total shift in the electron energy smaller. This result shows a good correspondence with the result of PES,[20] which reports no band bending in the *p*-type interface.

The localized polarization and electric field must involve a spatial charge distribution, which is given by the divergence of the electric field. As we follow the polarization from the LAO side to the STO side, a sharp increase in the polarization is found at the interface. This means that a significant amount of charge is distributed at the interface. Since the polarization in the *p*-type sample decays within a few unit cells, there is a large amount of charge in this thin region. In addition, these charges should not be mobile because the *p*-type interface is insulating. A possible source of such immobile charge at the interface is cation deficiencies,

because the electric field in the STO region estimated by the anion/cation displacement is inward and negative charge is expected to screen this electric field. The cation vacancies are robust to oxygen annealing at the relatively low growth and annealing temperature, in good correspondence to the negligible effect of oxygen annealing on the p -type interface conductivity. In the n -type sample, the polarized region is widely spread in the STO side, implying a relatively low charge density spread over a thicker region. This result coincides with experimentally reported carrier distribution profiles of the mobile electrons[21–24], emphasizing the difference in screening of the electrons and the ionic vacancies.

In conclusion, our structural investigation into the two types of LAO/STO interfaces reveals a clear difference in the polarization between the n -type and the p -type interfaces. The contrasting polarized structures are understood by considerable ionic vacancies in the p -type interfacial (over three to four layers), compared to the polarization screening by the electrons in the n -type case.

This work was supported by the TORAY Science Foundation and the Support Center for Advanced Telecommunications Technology Research. This work was also supported by KAKENHI (21740274,19052002) and the Global COE Program (G10). HYH acknowledges funding from the Department of Energy, Office of Basic Energy Sciences, Division of Materials Sciences and Engineering, under contract DE-AC02-76SF00515.

-
- [1] A. Ohtomo and H.Y. Hwang, *Nature* **427**, 423 (2004).
 - [2] N. Reyren *et al.*, *Science* **317**, 1196 (2007).
 - [3] H. Alves, A. S. Molinari, H. Xie and A. F. Morpurgo, *Nature Materials* **7**, 574 (2008).
 - [4] M. Huijben, A. Brinkman, G. Koster, G. Rijnders, H. Hilgenkamp and H. A. Blank, *Adv. Mater.* **21**, 1665 (2009).
 - [5] S. Thiel G. Hammerl, A. Schmehl, C.W. Schneider, and J. Mannhart, *Science*, **313**, 1942 (2006).
 - [6] H.Y. Hwang, *Science*, **313**, 1895 (2006).
 - [7] Y. Segal, J. H. Ngai, J. W. Reiner, F. J. Walker, and C. H. Ahn, *Phys. Rev. B* **80**, 241107R (2009).
 - [8] R. Pentcheva and W.E. Pickett, *Phys. Rev. Lett.* **102**, 107602 (2009).

- [9] U. Schwingenschloegl and C. Schuster, Europhysics Letters **86**, 27005 (2009).
- [10] Z.S. Popović, S. Satpathy, and R.M. Martin, Phys. Rev. Lett. **101**, 256801 (2008).
- [11] M.S. Park, S. H. Rhim, and A.J. Freeman, Phys. Rev. B, **74**, 205416 (2006).
- [12] For a classic example, I. K. Robinson, R. T. Tung, and R. Feidenhans'l, Phys. Rev. B **38**, 3632 (1988).
- [13] Y. Yacoby *et al.*, Nature Materials **1** 99, (2002).
- [14] P. R. Willmott *et al.*, Phys. Rev. Lett. **99**, 155502 (2007).
- [15] N. Nakagawa, H.Y. Hwang and D.A. Muller, Nature Materials, **5**, 204 (2006).
- [16] T. Ohnishi, M. Lippmaa, T. Yamamoto, S. Meguro and H. Koinuma, Appl. Phys. Lett. **87**, 241919 (2005).
- [17] T. Ohnishi, K. Shibuya, M. Lippmaa, D. Kobayashi, H. Kumigashira, M. Oshima and H. Koinuma, Appl. Phys. Lett. **85**, 272 (2004).
- [18] S. A. Pauli *et al.*, Phys. Rev. Lett. **106**, 036101 (2011).
- [19] See EPAPS document number ### for the structural buckling of each layers in the *n*- and *p*-type interface.
- [20] K. Yoshimatsu, R. Yasuhara, H. Kumigashira, and M. Oshima, Phys. Rev. Lett. **101**, 026802 (2008).
- [21] N. Reyren, S. Gariglio, A. D. Caviglia, D. Jaccard, T. Schneider, and J.-M. Triscone, Appl. Phys. Lett. **94**, 112506 (2009)
- [22] C. Bell *et al.*, Phys. Rev. Lett. **103**, 226802 (2009).
- [23] O. Copie *et al.*, Phys. Rev. Lett. **102**, 216804 (2009).
- [24] A. Dubroka *et al.*, Phys. Rev. Lett. **104**, 156807 (2010).